DAMPING PROPERTIES OF SEQUOIA AND BIRCH UNDER SHOCK LOADING

A.P.Bolshakov, N.N.Gerdjukov, E.V.Zotov,
S.A.Novikov, V.A.Sinitsin, Yu.I.Scherbak

VNIIEF - RFNC, Russia, 607190, Sarov, Nizhni Novgorod region

ABSTRACT

To decrease mechanic effect on loads being transported, shock load limiters (dampers) are being widely used today. Usually, the materials having «stress-strain» diagrams (σ-ε) of compression with a substantial portion, where σ=const, are used as dampers. Most widely used are dampers made of foam polystyrene having just the same compression diagram. Similar strain diagrams can be enlisted for some porous materials, timber under cross compression, perforated metallic crushers and some others. By selecting damper material, the level of transmitted to the protected object pressures can be varied from several to hundreds MPa. Timber, as being widely used and featuring good technologic properties together with low cost, becomes an attractive material to be used as the limiter of shock loads.

This paper presents the results of stress - strain sequoia properties (USA deliverable) and birch properties (Volgo-Vyatski region) at dynamic (v=10m/s) and quasistatic ($v \cong 10^{-4}$m/s) loading rates. The samples (∅25x25mm) cut at 0, 5, 10, 15, 30, 45 and 90^0 angle relative to their fibre were tested on one-axis compression at -30, +20 and +65^{0}C and fixed humidity (ω = 6-7%). Dynamic tests employed Kolsky method performed at the facility including Hopkinson's compound rod (Zukas et al.,1985). Sample loading was executed by trapezoidal pulsed pressure created by the explosive device. Samples were heated and cooled by special thermostates.

DYNAMIC TESTING METHOD

The major parts of experimental facility for sample dynamic tests (fig.1) are: explosive loading device, two measuring rods with the sample being tested and measuring/computation complex (MCC). The samples are tested in lab. The explosive device consists of the ampule with high explosive (HE) (6), metallic stricker (7) and perforated aluminium crusher (10). It is located inside small-size metallic chamber (1). Pressure pulse of the required amplitude (≅ 0.2MPa) and duration (≅200ms) is created by explosion of a small mass charge (0.75g total), liquid high explosive (LHE) with help of massive metal support (3a, b).

The LHE charge (Zotov et al.,1982) is initiated by sparkle discharger (8) after the high-voltage pulse has been sent to it from the high-voltage facility (17). Coordination of LHE explosion with the recorder start-up is performed by synchronizing unit (18). Tests with low (-30^{0}C) and high (+65^{0}C) temperatures employ special thermostates (14) where the samples are conserved. Conservation time is not less than 1 hour.

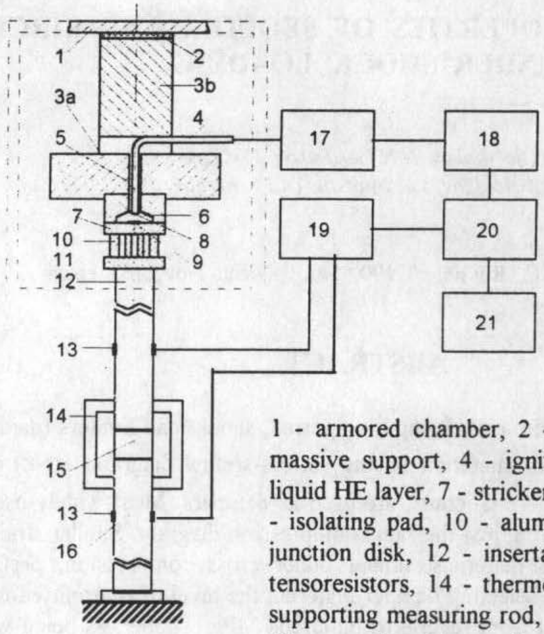

1 - armored chamber, 2 - rubber damper, 3a, b - massive support, 4 - ignition cable, 5 - HE inlet, liquid HE layer, 7 - stricker, 8 - sparkle discharger, 9 - isolating pad, 10 - aluminium perfocrusher, 11 - junction disk, 12 - insertable measuring rod, 13 - tensoresistors, 14 - thermostate, 15 - sample, 16 - supporting measuring rod, 17 - high voltage facility, 18 - synchronizing unit, 19 - tensostation, 20 - SAMAS recorder, 21 - PC.

Fig.1. Schematic layout of measuring/computation complex.

Signals from tensogauges (13) are recorded by tensostation (19) having digital recorder (20) controlled by PC (21). Information from the tensogauges is transmitted to a diskette for the further processing.

In each experiment two files of electric voltage values in volts ($U_{\varepsilon_I}, U_{\varepsilon_T}$) were obtained from tensogauges. Being recorded on diskettes, the files corresponded to the values of strain in loadin (ε_I) and passing (ε_T) waves of stress, recorded in certain scale (see fig.2).

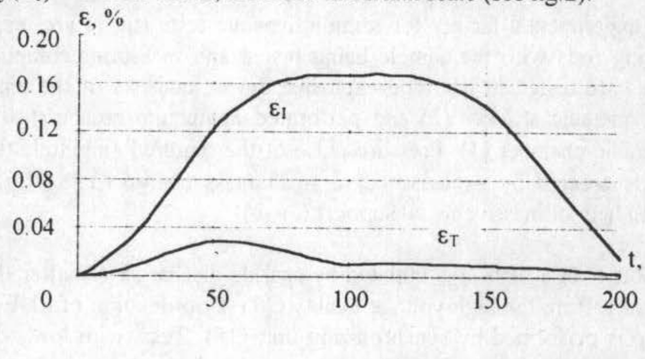

Fig.2. Recording of strains in loading (ε_I) and passing (ε_T) waves of stress.

Mathemathic processing of experimental data involved:

1. Creation of mathemathic code to calculate pares of σ_k and ε_k values (k=1, 2, 3...) using measured strain values $\varepsilon_I(t)$ and $\varepsilon_T(t)$;
2. Making plots of «stress vs time» $\sigma(t)$, «strain vs time» $\varepsilon(t)$ and, finally, «strain-stress» «σ-ε» at specified strain rate $\dot{\varepsilon}$.

Strains of insertable ($\varepsilon_T(t)$) and supporting ($\varepsilon_T(t)$) rods, measured in the experiment, were used to determine stress σ_S and strain ε_S of the sample with help of the following expressions (Bolshakov et al., 1989):

$$\sigma_s(t) = \varepsilon_T(t)E \cdot \frac{F_c}{F_o}, \tag{1}$$

$$\varepsilon_s(t) = \frac{2a}{l}\int_0^t [\varepsilon_I(t) - \varepsilon_T(t)]dt \tag{2}$$

where F_C and F_0 - the rod and the sample cross-section areas, correspondingly, a - the rate of elastic waves distribution in the rod, E - the rod material elasticity modulus, l - the sample length.

The sample loading rate v was determined by maximum stress σ_m value in compression loading wave from the formulation:

$$v = \sigma_m / \rho\, a, \tag{3}$$

where ρ - the rod material density.

Provided by precise dosage of LHE, maximum loading σ_m value repeated regularly from test to test. It was 255±5MPa. That is why sample loading rate v was also constant, v=10m/s. Tests at quasistatic loadings ($v \cong 10^{-4}$m/s) were performed at the breaking machine R-5 using thermostates to provide the required temperature. Experimental results in the form of «σ-ε» dynamic diagrams, obtained from the samples taken from the middle parts of sequoia and birch with different angles of fibre orientation α, are presented in fig. 3(a, b).

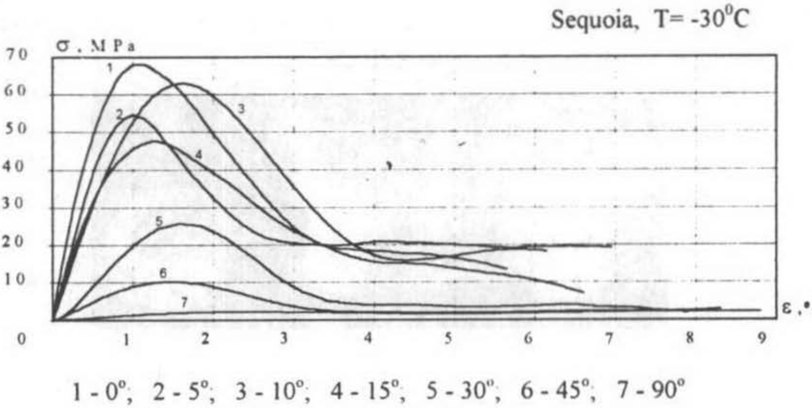

Fig. 3 a. Dynamic «σ-ε» diagrams for sequoia.

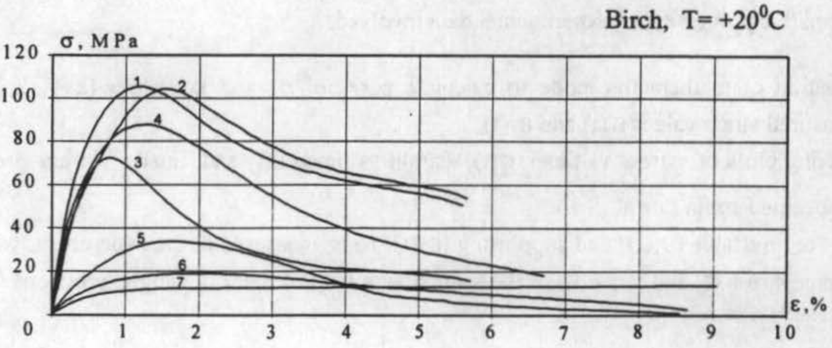

1 - 0°; 2 - 5°; 3 - 10°; 4 - 15°; 5 - 30°; 6 - 45°; 7 - 90°.

Fig. 3 b. Dynamic «σ-ε» diagrams for birch.

Diagrams of sample deformation under quasistatic loading are of the similar nature. The main phenomenon differentiating the dynamic diagrams from the quasistatic ones is notably lower (1.5 to 2 times) value of fracture deformation ε_P (σ_{comp} = max), which, once having been achieved, signalled the beginning of sample fracture. Strain diagrams «σ-ε» of the samples with fibre angles α=5, 10, 15, 30 and 45^0 relative to loading vector are of a similar nature to the diagrams for samples having $\alpha=0^0$. The only difference is a substantial decrease of rupturing stress value (from 10-20% to 6-10 times) associated with an orientation angle increase from 5 to 45^0. For sequoia and birch samples with α=0, 5, 10 and 15^0 it is typical form of cracks at maximum stress (fracture stress σ_{comp}) and further crack propagation along the entire sample with significant fall of stress (see fig. 4). Stress σ_{comp} at sectional compression ($\alpha=0^0$) for both sequoia and birch samples had approximately the same constant values up to strains ε=30-40% where layer repacking starts. Sample deformation here is accompanied by chipping and fibre fracture. Formation of shearings under the same angles is typical for destruction of samples with orientation angles α=30 and 45^0. At sectional compression ($\alpha=90^0$) sample fracturing into several parts has not been observed. We have observed declination of annual rings, that is repacking, and the associated decrease of sample thickness up to ≈50%. Both sequoia and birch samples with $\alpha=0\div45^0$ rupture at strain values ε=1-3%.

α=0, 5, 10, 15° α=30, 45° α=90°

Fig. 4. Types of fracture of the samples with different orientation angles α.

Strength limit σ_{comp} values for sequoia and birch at different α angles are listed in Tables 1,2.

Table 1.

Dynamic and quasistatic strength of sequoia samples depending on fibre orientation angle and temperature

Orient. angle α	Timber density ρ, kg/m^3	Strength limit σ_{comp}, MPa						Fracture deformation ε_d, %					
		-30 °C		+20 °C		+65 °C		-30 °C		+20 °C		+65 °C	
		σ^d_c	σ^{ST}_c	σ^d_c	σ^{ST}_c	σ^d_c	σ^{ST}_c	ε^d_d	ε^{ST}_d	ε^d_d	ε^{ST}_d	ε^d_d	ε^{ST}_d
0	418	68	51	40,2	48	55,3	56	1,1	2,6	1,4	3,3	1,4	3,3
5	405	54,5	53	37,1	50	47,4	49	1	2,4	1,2	2,7	1,4	3,2
10	408	63	43	43,3	48	48,7	45	1,6	2	1,6	3	1,2	2,9
15	417	47,7	40	45,3	36	27	38	1,3	2	1,6	1,6	0,5	1,8
30	412	25,7	16	26,8	21	17,7	18	1,6	1,7	1	1,7	1,1	2,2
45	370	10,1	8	11,4	9	13,1	8	1,4	2,2	1,4	2,2	0,6	1
90	420	2	3,8	4	3,7	3	3,7	-	33	-	36	-	31
	$\rho_{mid.}$=407												

Table 2.

Dynamic and quasistatic strength of birch samples depending on fibre orientation angle and temperature

Orient. angle α	Timber density ρ, kg/m^3	Strength limit σ_{comp}, MPa						Fracture deformation ε_d, %					
		-30 °C		+20 °C		+65 °C		-30 °C		+20 °C		+65 °C	
		σ^d_c	σ^{ST}_c	σ^d_c	σ^{ST}_c	σ^d_c	σ^{ST}_c	ε^d_d	ε^{ST}_d	ε^d_d	ε^{ST}_d	ε^d_d	ε^{ST}_d
0	624	128	88	105	81	104	86	1,5	2,7	1,3	2,1	1,6	2,4
5	600	119	85	108	81	94	78	1,1	1,4	1,4	1,6	1,8	1,9
10	603	57	65	77	65	61	58	1,1	1,7	1,1	2,8	1,6	2,9
15	627	65	71	81	66	68	74	1,5	1,6	1,4	3,4	1,2	2
30	633	34	38	35	35	32	35	1,5	3,3	1,7	4,2	1,5	3,6
45	609	17	24	19	23	18	16	2,6	2,8	2	4,6	1,7	2,7
90	590	8	12	12	11	10	10	-	32	-	41	-	38
	$\rho_{mid.}$=612												

Strength σ_{comp} vs orientation angle α is shown graphically in fig.5 with sequoia as an example.

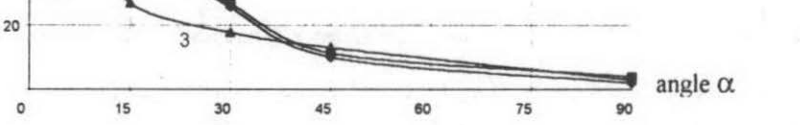

Fig.5. Sequoia strength σ_{comp} vs angle α and temperature.

Maximum stress values of sectional compression (α=90^0) for the tested samples are less than fracture stresses of the longitudinal one (α=0^0) approximately in order. Loading rate effect on timber strength was observed only for birch samples with cutting angles α=0 and 5^0 at temperature T=-30^{0}C (dynamic strength increased up to 30%). From experimental results it can be noted that timber strength at the increased temperatures T=65^{0}C is lower, as a rule, than at the lower temperatures, and birch strength σ_{comp} is higher than that of sequoia in 1.5-2 times at any fibre orientation angles relative to loading vector.

The experiments were executed within AJ-286 Contract with Sandia National Laboratories (SNL), Albuquerque, NM, USA.

Special thanks to Senkova S.V. for a great job of data processing and issue of documents.

RESUME

We have accomplished a study of damping properties (strain-stress) of sequoia and birch timber at different temperatures and fibre orientation angle relative to loading direction at dynamic (v=10m/s) and quasistatic (v$\cong$10^{-4}m/s) compression. All the tests were performed at constant humidity ω=6-7%.

The results of the above tests were used to construct strain diagrams «σ-ε» for sequoia and birch samples with α=0, 5, 10, 15, 30, 45 and 90^0 at two loading modes (v=10m/s and v $\cong$ 10^{-4}m/s) and temperatures T=-30, +20 and +65^{0}C. Dependencies «σ-ε» at dynamic and quasistatic loading of sequoia and birch samples with α=0, 5, 10, 15, 30, and 45^0 have a ball-shaped form, and maximum stress values (σ_{comp} strength limit) decrease as the angle increased. Strain rate at which sample fracture was observed, comprised 1-3%. Maximum strength of sequoia and birch samples at sectional compressure (α=0^0) was 120-130MPa for birch and 68-70MPa for sequoia. When the angle α grows, timber strength for sectional compression (α=90^0) decreases and achieves its minimum value 10-14MPa for birch and 3-6MPa for sequoia. Sectional compression for both timber types takes place at nearly constant stress up to strain equal to 30-40%. At further sectional compression (>30-40%), quick growth of resistance against strain is observed. Notable effect of loading rate on timber strength was observed only for birch samples with orientation angles α=0 and 5^0 at temperature T=-30^{0}C (dynamic ratio approximately equal to 1, 3).

REFERENCES

Zukas J.A., Niskolas T., Swift H.F. and others.Shock dynamics (transl. from English)., Mir, 1985.

Zotov E.V. Kozyrev A.S., Babadej S.M. and others. Initiation of detonation of nitrobenzene solutions in tetranitromethane in the electric discharge channel. FGV, 1982, N° 4.

Bolshakov A.P.. Novikov S.A,. Sinitsin V.A. Strength of constructional materials under dynamic loads (review), VANT, series: Physics and technics of nuclear reactors, 1989, iss. 1.